



1

2 Seasonal Variation of Total Column Formaldehyde, Nitrogen Dioxide, and Ozone Over Various Pandora  
3 Spectrometer Sites with a Comparison of OMI and Diurnally Varying DSCOVR-EPIC Satellite Data

4

5

6 Jay Herman<sup>1</sup> and Jianping Mao<sup>2</sup>

7

8

9

10

11

12

13

14

15

16

17

18

19

20

21 <sup>1</sup>GESTAR II University of Maryland Baltimore County, Baltimore, Maryland USA

22 (herman@umbc.edu)

23 <sup>2</sup>University of Maryland, College Park, MD 20740, USA ([jianping.mao@nasa.gov](mailto:jianping.mao@nasa.gov))

24

25

26

27

28



29

## 30 Abstract

31 Both The OMI (Ozone Monitoring Instrument) satellite and the Pandora ground-based instruments  
32 operate with spectrometers that have similar characteristics in wavelength range and spectral resolution  
33 that enable them to retrieve total column amounts of formaldehyde TCHCHO, and nitrogen dioxide  
34 TCNO<sub>2</sub>, and ozone TCO at 13:30 ± 0:45 local time. At most sites, Pandora shows a strong seasonal  
35 dependence for TCO and TCHCHO and little seasonal dependence for TCNO<sub>2</sub>, while OMI sees little  
36 seasonal dependence for TCHCHO and TCNO<sub>2</sub> but does see the seasonal dependence for TCO. The  
37 seasonal behavior of TCHCHO is caused by plant growth and emissions from lakes that peak in the  
38 summer suggesting that OMI is not correctly retrieving TCHCHO all the way to the Earth's boundary  
39 layer. Since the OMI retrieval is around 13:30 local equator crossing time ± 0:45 and tends to occur near  
40 the frequent minimum of the daily TCNO<sub>2</sub> time series, OMI underestimates the amount of air-pollution  
41 that occurs during each year. Better TCNO<sub>2</sub> agreement occurs when the Pandora data is averaged  
42 between 13:00 and 14:00 hours local time. Comparisons of OMI total column NO<sub>2</sub> and HCHO with  
43 Pandora daily time series show both agreement and disagreement at various sites and days. Similar  
44 comparisons of OMI TCO with those retrieved by Pandora show good agreement in most cases.  
45 Additional comparisons are shown of Pandora TCO with hourly retrievals during a day from EPIC (Earth  
46 Polychromatic Imaging Camera) spacecraft instrument orbiting the Earth-Sun Lagrange point L<sub>1</sub>.

## 47 1.0 Introduction

48 Formaldehyde, HCHO, is ubiquitous in the atmosphere and as with other VOCs (Volatile Organic  
49 Compounds) are emitted from natural and anthropogenic sources, such as plants, animals, biomass  
50 burning, fossil fuel combustion, and industrial processes (Zhang et al., 2019; Morfopoulos et al., 2021).  
51 Formaldehyde is mainly produced from the oxidation of VOCs such as isoprene, methane, and  
52 anthropogenic emissions (Wittrock, 2006). Formaldehyde can also be directly emitted from some  
53 sources, such as vehicle exhaust, tobacco smoke, building materials, and wood burning affecting  
54 pollution levels both indoors and outdoors. The majority of gaseous and atmospheric formaldehyde  
55 derive from microbial and plant decomposition (Peng et al., 2022). HCHO concentrations in the first few  
56 kilometers of the atmosphere vary depending on the location, time of day, season, and meteorological  
57 conditions. Some of the factors that influence total atmospheric column amounts of HCHO are:

- 58 • **Solar radiation:** Formaldehyde is photolyzed by solar ultraviolet radiation, which means it is broken  
59 down into smaller molecules and radicals. The photolysis rate of formaldehyde depends on the solar  
60 zenith angle, the cloud cover, and the atmospheric composition. Generally, formaldehyde photolysis  
61 is faster during mid-day and in the summer.
- 62 • **Temperature:** The thermal decomposition rate of formaldehyde increases with temperature, which  
63 means it is faster in warmer regions and seasons.
- 64 • **Humidity:** Formaldehyde reacts with water vapor in the atmosphere, forming formic acid and  
65 hydroxyl radicals. The reaction rate of formaldehyde with water vapor depends on the relative  
66 humidity, which varies with the temperature and the precipitation. Generally, formaldehyde  
67 reaction with water vapor is faster in humid regions and seasons.

68  
69 The largest sources of NO<sub>2</sub> are obtained from fossil fuel burning from various types of automobiles truck  
70 emissions and power generation (Van der A, 2008; Stavrou et al. 2020) followed by industrial



71 processes and oil and gas production. Additional sources are soils under natural vegetation and the  
72 oceans, agriculture and the use of nitrogen rich fertilizers, forest fires, and lightning. In populated areas,  
73 anthropogenic sources of lower tropospheric NO<sub>2</sub> are larger than natural sources. Nitrogen oxides play a  
74 major role in atmospheric chemistry and the production and destruction of ozone in both the  
75 troposphere and stratosphere. In the boundary layer high concentrations of both HCHO and NO<sub>2</sub> are  
76 health hazards for humans.

77

78 HCHO, NO<sub>2</sub> and O<sub>3</sub> in the atmosphere are typically measured by several types of instruments.

79 • Airborne: The GeoTASO instrument is a spectrometer that measures formaldehyde and other trace  
80 gases from an aircraft. The GeoTASO data can be used to validate and improve the satellite  
81 retrievals of formaldehyde and to study the emission sources and transport processes of  
82 formaldehyde in the atmosphere (Judd et al., 2018).

83 • Satellite: The Ozone Monitoring Instrument (OMI) is a satellite sensor launched in July 2004 that  
84 measures HCHO, NO<sub>2</sub>, O<sub>3</sub>, and other atmospheric constituents from space. The OMI data can be  
85 used to monitor their global distribution and long-term trends, and to investigate the role of NO<sub>2</sub>  
86 and HCHO in atmospheric chemistry and air quality (Boeke et al., 2011). For ozone, DSCOVR (Deep  
87 Space Climate Observatory), located at the Earth-Sun gravitational balance Lagrange point L<sub>1</sub>,  
88 contains a filter-based instrument EPIC (Earth Polychromatic Imaging Camera) capable of obtaining  
89 TCO once per hour (90 minutes in Northern hemisphere winter) simultaneously at 18 x 18 km<sup>2</sup>  
90 resolution for the entire sunlit globe at the Earth rotates (Herman et al., 2018). Other current  
91 satellite instruments also detect NO<sub>2</sub> and HCHO, such as The TROPOspheric Monitoring Instrument  
92 (TROPOMI).

93 • Ground-based Spectrometer: The Pandora spectrometer system forms a worldwide network of 67  
94 direct sun observing instruments that match atmospheric observations with known laboratory  
95 spectra of HCHO, NO<sub>2</sub>, and O<sub>3</sub> to obtain the total vertical column above the Pandora instrument  
96 every 2 minutes. Pandora uses a single-grating spectrometer and a charge-coupled device (CCD)  
97 2048 x 64-pixel detector to record the direct-sun spectra in the ultraviolet and visible wavelength  
98 range, 280 – 525 nm with an oversampled 0.5 nm spectral resolution. The retrieval algorithm is  
99 based on a spectral fitting technique to retrieve the slant column densities of HCHO, NO<sub>2</sub> and other  
100 gases, and then convert them to vertical column densities using geometric air mass factors  
101 appropriate for direct-sun observations. Pandora spectrometers have been deployed in various field  
102 campaigns and locations to monitor the spatial and temporal variability of TCHCHO and TCNO<sub>2</sub> to  
103 validate and improve the satellite observations of TCHCHO (Herman et al., 2009, Tzortziou et al.,  
104 2015, Spinei et al., 2018).

105

106 This study will examine the seasonal cycles of total column NO<sub>2</sub>, HCHO, and O<sub>3</sub> seen by the Pandora  
107 instruments by examining multi-year (2021 – 2024) time series for seasonal and daily behavior at various  
108 sites and will compare with observations made from the OMI satellite overpass measurements of the  
109 Pandora sites. Pandora ozone measurements will be additionally compared to hourly data obtained  
110 from EPIC. All of the Pandora data used in this study are after the upgrade of the instruments to  
111 eliminate internal sources of HCHO (Spinei, et al., 2021). Part of this study (TCNO<sub>2</sub> and TCO) is an  
112 extension of Herman et al. (2019) using Pandora data (2012 – 2017) before the internal upgrade.  
113 A difference is that Pandora TCO is now compared with hourly TCO retrieved by DSCOVR-EPIC.

114

115



116 **2.0 Examples of Seasonal and Daily Variation of HCHO and NO<sub>2</sub>**

117 Worldwide Pandora data for 147 sites can be downloaded from the Austrian Pandonia website  
 118 <https://data.pandonia-global-network.org/> or from a NASA backup site updated every week.  
 119 [https://avdc.gsfc.nasa.gov/pub/DSCOVER/Pandora/DATA\\_02/](https://avdc.gsfc.nasa.gov/pub/DSCOVER/Pandora/DATA_02/). Of interest for this study are the Level-2  
 120 (L2) time series ASCII files. For example, the Bronx New York City files for Pandora instrument 180 for  
 121 TCNO<sub>2</sub> data are in Pandora180s1\_BronxNY\_L2\_rnvs3p1-8.txt, TCHCHO in  
 122 Pandora180s1\_BronxNY\_L2\_rfus5p1-8.txt, and TCO data in Pandora180s1\_BronxNY\_L2\_rout2p1-8.txt.  
 123 The data are arranged in irregular columns that are identified in the metadata header for each file. In  
 124 the current version, column 1 contains the date and time for each measurement and column 39  
 125 contains measured column density in moles m<sup>-2</sup> (multiply by 6.02214076x10<sup>23</sup>/2.6867 x10<sup>20</sup>= 2241.4638  
 126 to convert to DU where 1 DU = 2.6867 x 10<sup>20</sup> molecules m<sup>-2</sup>). Pandora data also contain measurements of  
 127 water vapor, and SO<sub>2</sub> total column amounts.

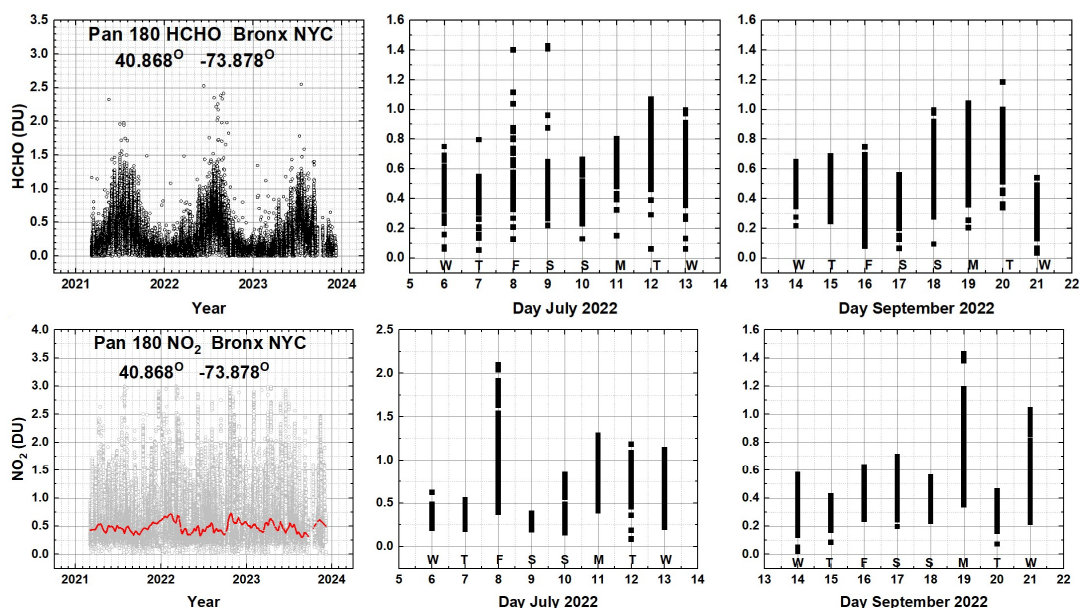


Fig. 01 Seasonal and daily behavior of HCHO and NO<sub>2</sub> from Pan 180 located in the Bronx, NYC at 40.868°N, -73.878°W. The red line is a Lowess(0.03) fit to the data, which is approximately a 1-month local least-squares average. The Local principal investigator for Pan 180 is Dr. Luke Valin.

128

129 Figure 1 shows the seasonal and daily variation of total column HCHO (TCHCHO) and NO<sub>2</sub> (TCNO<sub>2</sub>) using  
 130 all of the Pandora data obtained during each day in Bronx, New York. The daily data for 1 week in July  
 131 and September shows the range of values for both weekdays and weekends. When all the TCHCHO data  
 132 are plotted as an aggregate for 3 years, there is a strong seasonal pattern with a maximum in July and a  
 133 minimum near the end of December. The summer seasonal dependence of TCHCO is consistent with the  
 134 surface HCHO values observed by the ground-based Air-Quality System AQS (Wang et al., 2022). For  
 135 TCNO<sub>2</sub>, there is only a weak seasonal pattern with small maxima in January-February, since the sources  
 136 of NO<sub>2</sub> are largely from the nearly constant flow of cars and trucks.





137 Figure 2 shows the daily average of Pandora data obtained from diurnal variation of TCHCHO and TCNO<sub>2</sub>  
 138 from 09:00 to 15:00 local standard time (GMT – 5) (Pandora180s1\_BronxNY\_L2\_rfus5p1-8.txt). The  
 139 primary emission sources of atmospheric HCHO include direct emission from vegetation, the soil,  
 140 biomass burning, and decaying plant and animal matter. This is consistent with the Bronx location that is  
 141 adjacent to a large, vegetated park with a small lake near Fordham University. The same seasonal  
 142 dependence and magnitude occurs when the Pandora sampling is restricted to 13:00 to 14:00 local  
 143 standard time similar to the OMI overpass time.

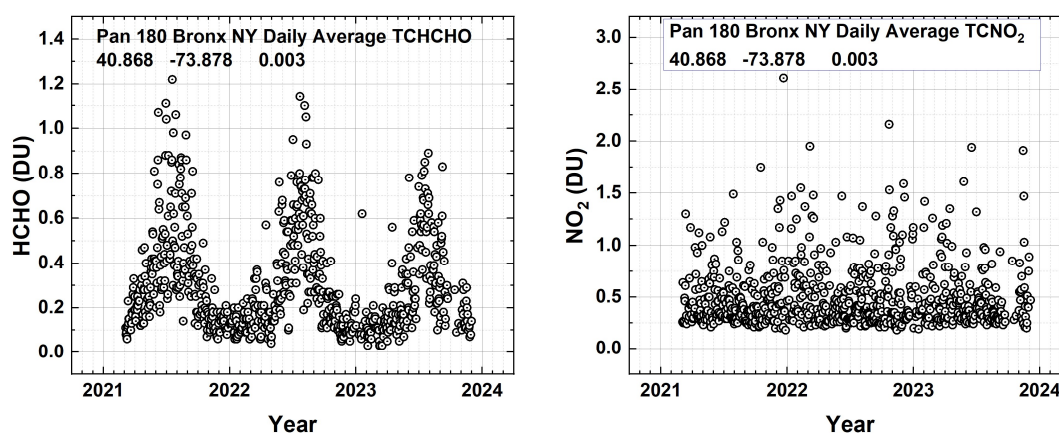


Fig. 02 The daily average seasonal variation of HCHO and NO<sub>2</sub> over Fordham University in Bronx, New York City from Pandora 180 at 40.868° latitude and -73.878° longitude. Each point is a daily average of the data in Fig.1. Local principal investigator: Dr. Luke Valin

144

145 There are 3 Pandora sites in New York City and one in nearby Bayonne, New Jersey. The NYC sites are in  
 146 the Bronx-Fordham University, Manhattan-City College NY (CCNY), Queens-Queens College. All four  
 147 successfully measure NO<sub>2</sub> in the period 2021 – 2023. A strong seasonal cycle in TCNO<sub>2</sub> is not seen (Figs.  
 148 1 and 2) in the traffic driven production of NO<sub>2</sub> in the Bronx, New York. The mean values of total column  
 149 NO<sub>2</sub> (TCNO<sub>2</sub>) for each the 3 New York sites are 0.5 DU while the TCNO<sub>2</sub> for the port city of Bayonne, NJ  
 150 is substantially higher at 0.7 DU. None of the four sites show any seasonal TCNO<sub>2</sub> pattern. For TCHCHO,  
 151 all four sites show an annual seasonal cycle with three of the sites having a 3-year average of 0.3 DU  
 152 except for the Queens site at 0.45 DU. The Queens site may be anomalous because of many missing  
 153 points affecting the average.

154 Similar behavior is seen at other sites such as the one from New Haven Connecticut located in a  
 155 vegetated area adjacent to two rivers (Fig.3). TCHCHO has a clear summer peak in June – July and a  
 156 suggestion of a winter TCNO<sub>2</sub> peak in December – January coinciding with the maximum heating  
 157 season.

158 The seasonal variation of TCHCHO could not be studied prior to the internal upgrade of Pandora after  
 159 2019 that was needed because of the release of HCHO from polyoxymethylene (POM-H Delrin) out-  
 160 gassing as a function of daytime temperature within the Pandora sun-pointing head (Spinei et al., 2021)

161

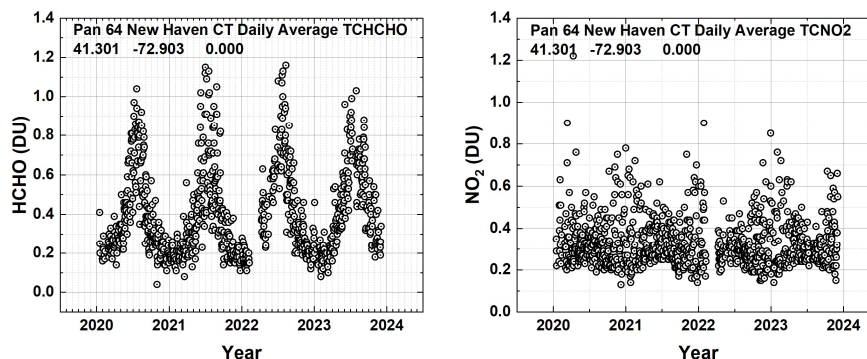


Fig. 03 The seasonal variation of TCHCHO and TCNO2 over New Haven Connecticut from Pandora 64 at 41.301°N latitude and -72.903°W longitude. Each point is a daily average. Local principal investigator: Dr. Nader Abuhassan

162

163 An equatorial Pandora site (Fig. 4) with a sufficiently long data record is located in Bangkok, Indonesia  
164 near a small park and lake. Bangkok has a tropical monsoon climate with three main seasons: hot season  
165 from March to June, rainy season from July to October, and cool season between November and  
166 February. TCHCHO has a seasonal cycle peaking in March – April when the sun is nearly overhead and a  
167 minimum during the rainy season. TCNO2 has a clear seasonal cycle peaking in December – January and  
168 a minimum during the rainy season.

169

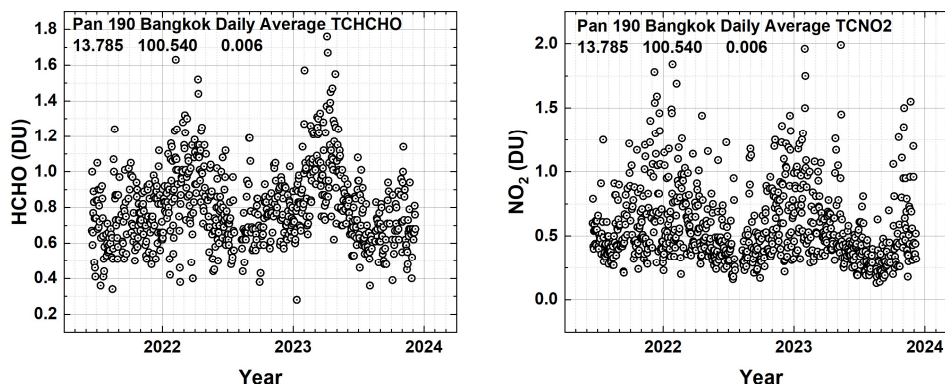


Fig. 04 The seasonal variation of TCHCHO and TCNO2 over equatorial Bangkok Indonesia at 13.785°N and 100.540°E. The local principal investigator is Surassawadee Phoornpanit.

170

171 An unusual counter example to the typical seasonal cycle is for the Pandora site located in Tel Aviv  
172 Israel. Tel Aviv has significant amounts of HCHO but does not show seasonal variation in TCHCHO  
173 because of a coastal location in a warm climate even at midlatitudes located at 32.113°N, 34.085°E that  
174 has essentially two seasons, a cool, rainy winter: October – April and a dry, hot summer: May –  
175 September. The result is there is limited seasonal increase in vegetational activity and no seasonal



176 variation in HCHO (Fig. 5). However, TCNO<sub>2</sub> shows a clear seasonal increase in the December - January  
177 months frequently reaching over 0.5DU. The TCNO<sub>2</sub> seasonality is similar to that of the near-surface  
178 concentrations reported by Boersma et al., (2009). The Pandora instrument 182 is located at Tel Aviv  
179 University about 1 km from a major highway. Tel Aviv has frequent episodes of smog associated with  
180 heavy automobile and truck traffic (Newmark, 2001).

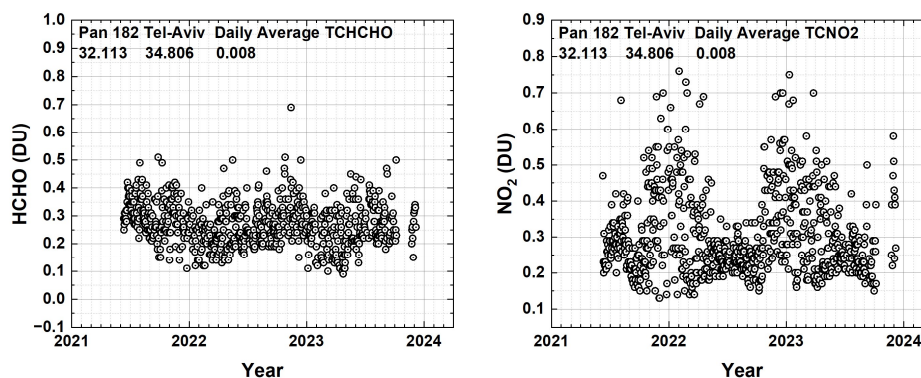


Fig. 05 Seasonal variation in daily average TCHCHO and TCNO<sub>2</sub> in Tel Aviv Israel from Pandora 182 located at 32.113°N, 34.085°E at a height of 8 meters. The local principal investigator for Pan 182 is Dr. Michal Rozenhaimer.

181

182 Finally, a Pandora example from the Southern Hemisphere SH from Wakkerstroom, South Africa located  
183 in a rural area near the ocean a few degrees outside of the equatorial zone at -27.359°S and 30.144°E.

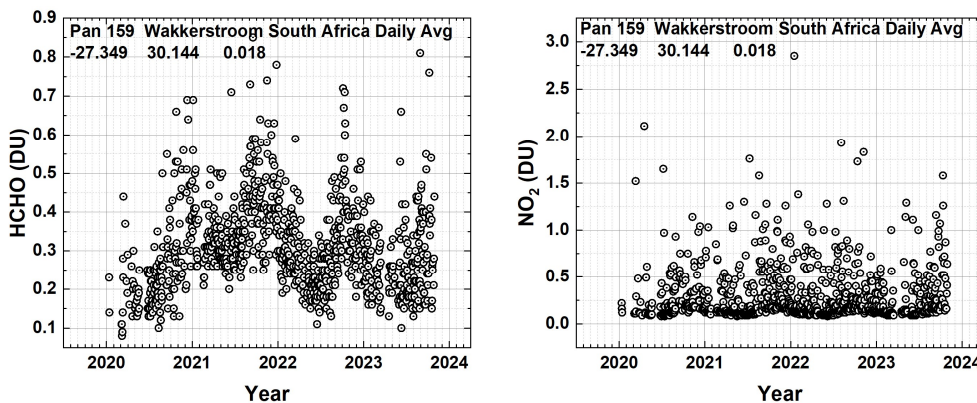


Fig. 06 Seasonal variation in daily average HCHO and NO<sub>2</sub> in Wakkerstroom South Africa from Pandora 159 located at -27.359°S and 30.144°E. Local principal investigator: B. Scholes

184

185 As expected, the peak value of TCHCHO occurs near the SH summer in November – December, while  
186 TCNO<sub>2</sub> has no significant seasonal dependence.

187



188 **2.1 Comparisons Between Pandora and OMI Retrievals of NO<sub>2</sub> and HCHO**

189 In this section two types of comparisons of Pandora with OMI satellite data are considered. The first is  
 190 the long-term TCNO<sub>2</sub> time series consisting of the data record of Pandora and OMI from 2020 – 2023.  
 191 The second looks at a few selected days and compares Pandora values with the mid-afternoon OMI  
 192 overpass at times near 13:30 hours equator crossing time. Pandora and OMI data are matched at the  
 193 same GMT and then converted to local solar time, GMT + Longitude/15. The OMI overpass HCHO and  
 194 NO<sub>2</sub> data are found at <https://avdc.gsfc.nasa.gov/pub/data/satellite/Aura/OMI/V03/L2OVP/OMHCHO/>.  
 195 <https://avdc.gsfc.nasa.gov/pub/data/satellite/Aura/OMI/V03/L2OVP/OMNO2/>

196

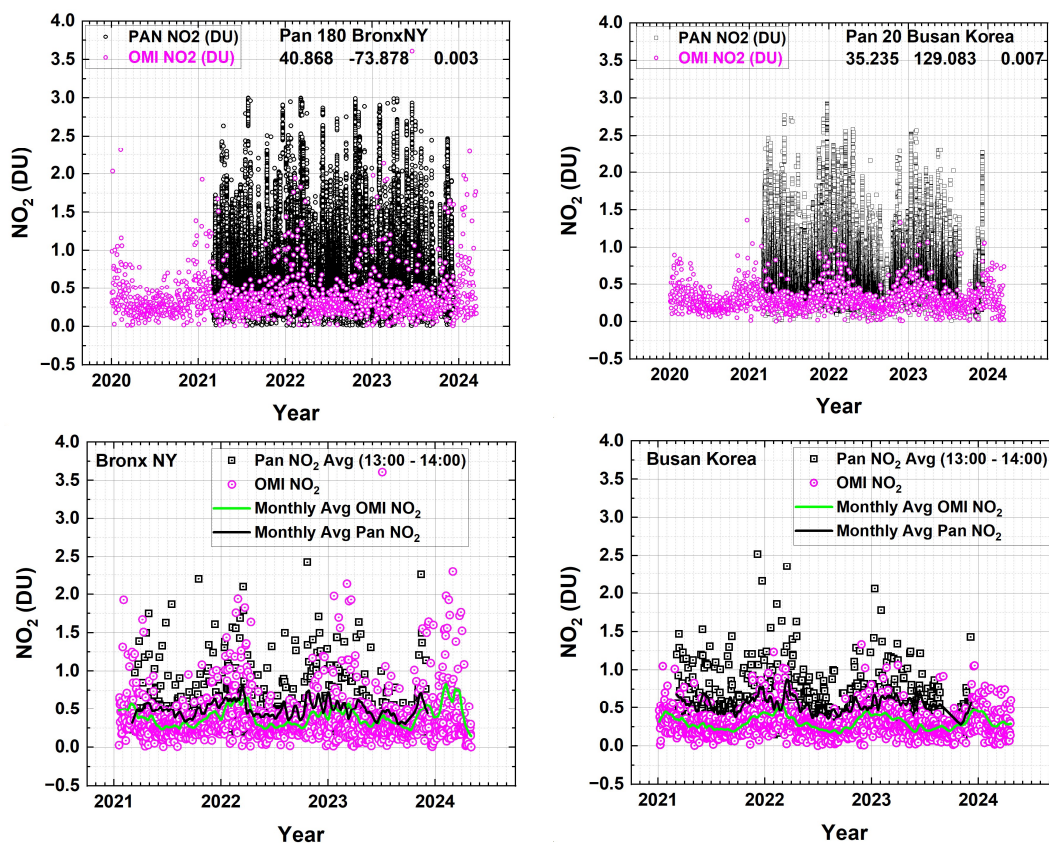


Fig. 07 Upper Panels: Comparison of OMI (approximately 13:30) and Pandora (09:00 – 16:00) total column NO<sub>2</sub> time series in Bronx NY (40.868°N, -73.878°W) and Busan Korea (35.235°N, 129.083°E). Lower Panels: Pandora averaged between 13:00 – 14:00 hours. Local principal investigator for Pan20 is Jae Hwan Kim and for Pan 180 is Dr. Luke Valin

197

198 Figure 7 illustrates that OMI only captures a fraction of the daily values of total column NO<sub>2</sub> and fails to  
 199 detect the extent of the daily pollution at both the Bronx New York City and Busan Korea sites. This is





200 because OMI and other polar orbiting satellites only collect data once per day (occasionally twice per day)  
 201 day) at any given location at mid-afternoon, frequently when TCNO<sub>2</sub> is below its daily maximum  
 202 (Herman et al., 2019). The lower panels of Fig. 7 show a comparison with OMI when Pandora data are  
 203 averaged between 13:00 and 14:00, which contains the OMI overpass time. This shows that OMI and  
 204 Pandora TCNO<sub>2</sub> agree more closely at the overpass time. The monthly average Pandora (13:00 to 14:00)  
 205 values are larger than those from OMI especially at Busan suggesting that the OMI field of view 13 x 24  
 206 km<sup>2</sup> may include areas of lower NO<sub>2</sub> values over the nearby ocean. In the case of the Bronx, the  
 207 differences are not statistically significant.

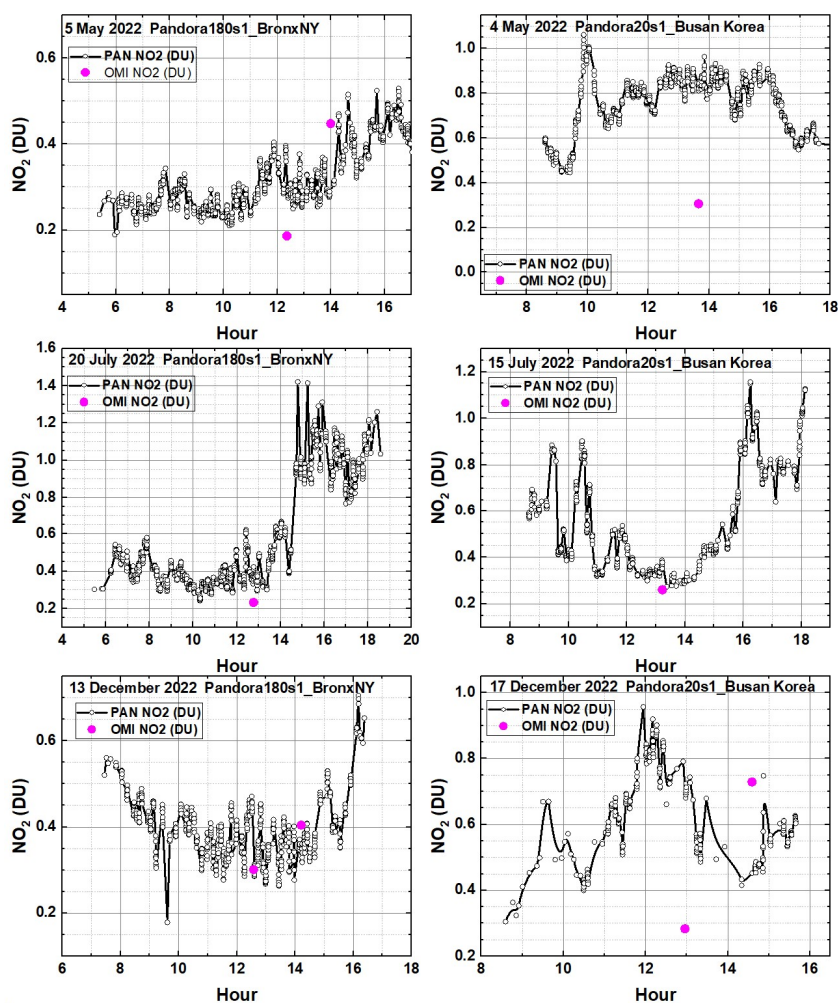


Fig. 08 A comparison between Pandora and OMI (purple circle) total column NO<sub>2</sub>. The Local principal investigator for Pan 180 is Dr. Luke Valin and for Pan 20 is Dr. Jae Hwan Kim.

208

209 Figures 8 and 9 show the diurnal daytime variation for 3 selected days for Pandora retrieved total  
 210 column NO<sub>2</sub> and HCHO compared with OMI at the overpass time for both Bronx New York City and



211 Busan Korea. These are typical examples of the highly variable hourly variation of TCHCHO and TCNO<sub>2</sub>  
 212 as observed by Pandora at most sites. The hourly variation of TCHCHO and TCNO<sub>2</sub> on any given day can  
 213 take on unique shapes depending on the presence of surface winds, changes in temperature, and  
 214 sunlight. The variability of TCNO<sub>2</sub> is also driven by the strength of the sources (automobile exhaust,  
 215 power generation, industry, etc.) as well as the meteorological conditions. Occasionally, there is good  
 216 agreement but in general the OMI overpass values do not agree with Pandora retrieved values for both  
 217 TCHCHO and TCNO<sub>2</sub>. In the sample shown in Figures 8 and 9, the cases of agreement are less than 50 %.

218

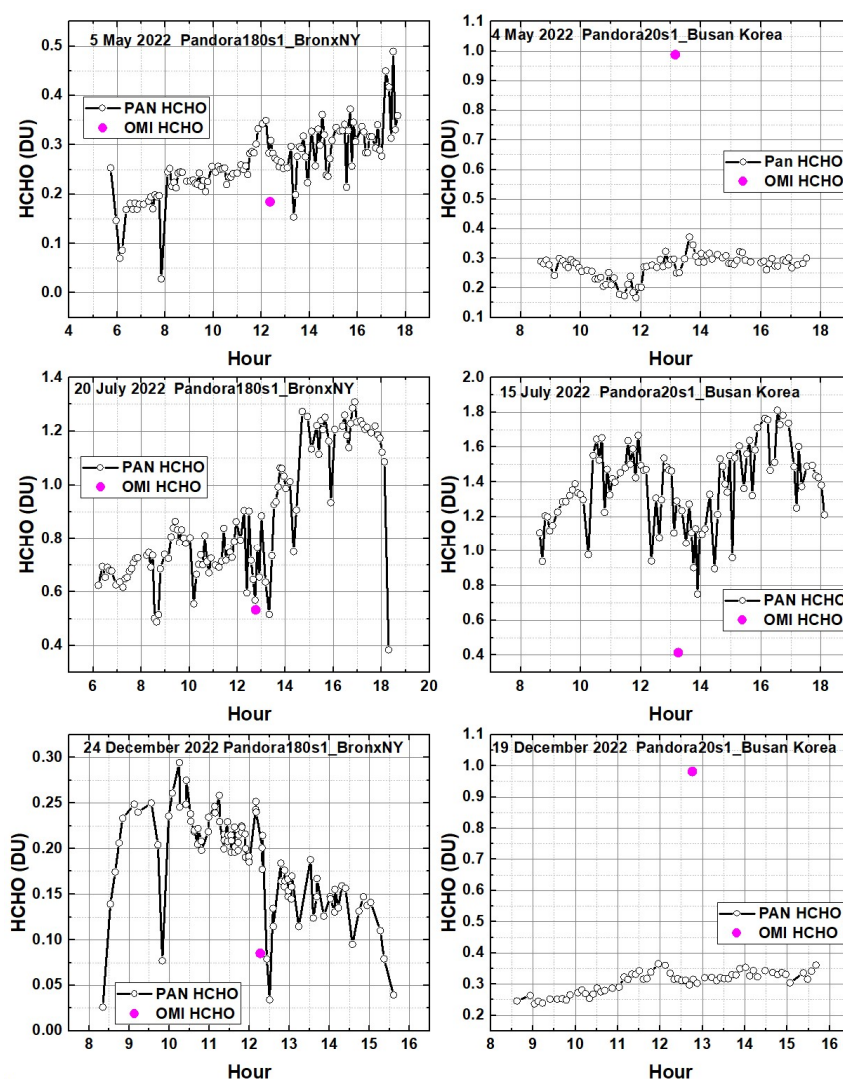


Fig. 09 A comparison between Pandora and OMI (purple circle) total column HCHO. The Local principal investigator for Pan 180 is Dr. Luke Valin and for Pan 20 is Dr. Jae Hwan Kim.

219



220 Figure 9 illustrates the comparison of TCHCHO retrievals from Pandora and OMI. The spectral fitting  
 221 algorithm for detecting HCHO absorption is in the same short wavelength UV spectral region as used for  
 222 ozone retrieval, 300 – 360 nm (Gratien et al. 2007). This means that the retrieval sensitivity for “seeing”  
 223 all the way to the surface is reduced. Also, small errors in ozone retrieval can affect the detection of  
 224 HCHO. This problem is not present for the spectral fitting of NO<sub>2</sub>, since that usually occurs in the visible  
 225 range 410 – 450 nm where there is only interference from a weak and narrow water vapor line.

226 Pandora TCHCHO daily average data (Fig. 10) for University of Toronto in Toronto-Scarborough (Lat =  
 227 43.784°N, Lon = -79.187°W) shows clear peaks in the summer from the vegetation in a surrounding park  
 228 area whereas TCNO<sub>2</sub> shows only small seasonal variation with small peaks also occurring in the summer  
 229 for values less than 0.4 DU. Higher values do not show any seasonal variation. The University of Toronto  
 230 is located near a major highway, which is a strong source of NO<sub>2</sub> from automobiles and trucks. Unlike  
 231 many sites, OMI TCHCHO data over Toronto East (centered on 43.74°N, -79.27°E about 8 km from the  
 232 Pandora site) also shows sporadic summer peak values that are higher than the Pandora daily averages  
 233 and all of the Pandora data (Fig. 10b).

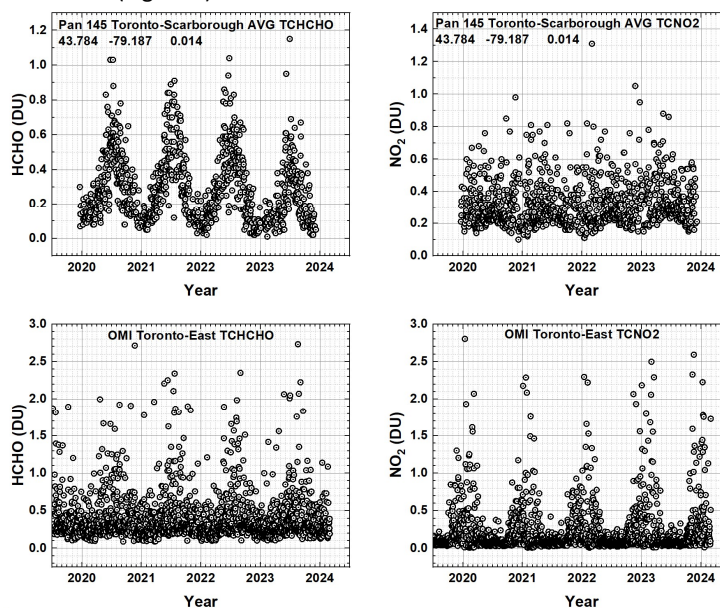


Fig. 10a A comparison of Pandora TCHCHO and TCNO<sub>2</sub> daily average total column amounts for Toronto-Scarborough University of Toronto and OMI data for Toronto East (43.740°N, -79.270°W at approximately 14:20 Local Standard Time). The local principal investigator for Pan 145 is Dr. Vitali Fioletov.

234

235 The Pandora site is in a park setting outside of Toronto while the nominal OMI Toronto East location and  
 236 OMI’s field of view includes the city. The OMI NO<sub>2</sub> amounts at 14:20 show a clear peak in December –  
 237 January corresponding to the peak winter heating for the city, while the remote Pandora site only shows  
 238 NO<sub>2</sub> from the highway traffic. HCHO peaks in June – July for both OMI and Pandora, but the Pandora  
 239 seasonal cycle is much stronger. Using all the Pandora data for Toronto-Scarborough (Fig.11), there is no  
 240 hint of an TCNO<sub>2</sub> annual cycle whereas the TCHCHO cycle is obvious with maximum values close to that  
 241 seen by OMI.





242

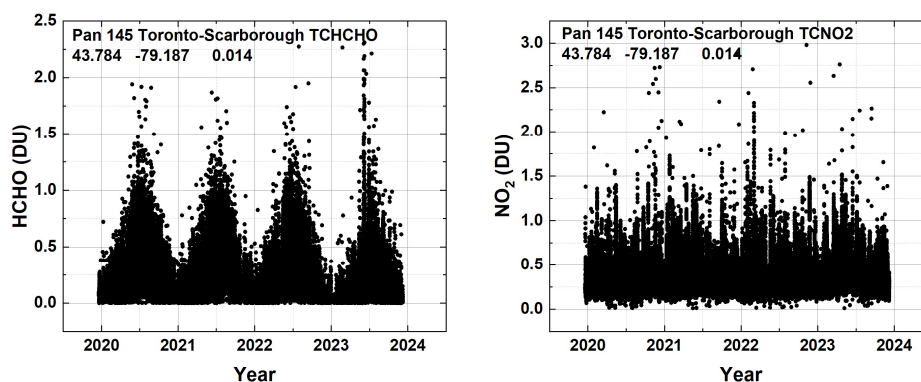


Fig. 10b The same as Fig. 10a but for all the Pandora 145 data.

243

244 **2.2 Total Ozone Column**

245 The retrieval of total column ozone amounts TCO serves as a check on the calibration of both OMI and  
 246 Pandora that is also needed for spectrally overlapping TCHCHO retrievals. Comparisons of Pandora TCO  
 247 with TCO measured by OMI show good agreement suggesting both instruments are well calibrated in  
 248 the UV range also needed for retrieving TCHCHO. The good TCO agreement is partly because most of the  
 249 O<sub>3</sub> is in the stratosphere near 25 km and the fact that ozone is slowly changing spatially over the OMI  
 250 field of regard for the overpass data. Figure 11 shows an example obtained over Washington DC from  
 251 the roof of the NASA Headquarters building and Fig. 12 is from the roof of a building at Pusan University,  
 252 Korea.

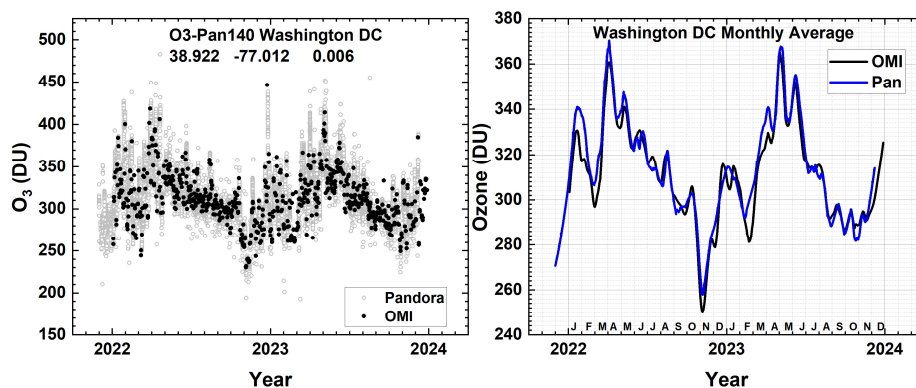


Fig. 11 A comparison of OMI Total Column Ozone values with those obtained from Pandora 140 over the Washington DC site at 38.922°N and -77.012°W. The local principal investigator for Pan 140 is Dr. Jim Szykman.

A test of Pandora UV data is a comparison between EPIC, OMI and Pandora TCO at the specific OMI and EPIC overpass times (Fig. 13a and 13b). that shows good agreement within 1 to 3 %. OMI TCO overpass data for all Pandora sites and more are available from <https://avdc.gsfc.nasa.gov/pub/data/satellite/Aura/OMI/V03/L2OVP/OMTO3/>

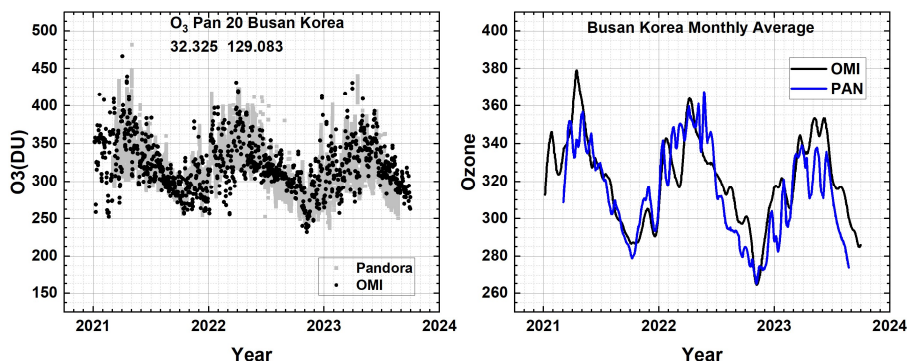


Fig. 12 A comparison of OMI Total Column Ozone values with those obtained from Pandora 20 over the Busan, Korea site at 32.325°N and 129.083°E. The local principal investigator for Pan20 is Jae Hwan Kim.

253 There is also good agreement between daily OMI TCO with that obtained from Pandora (Fig. 13a) at  
 254 most sites. The values obtained at Granada differ by about 8 DU or 2.8 %.

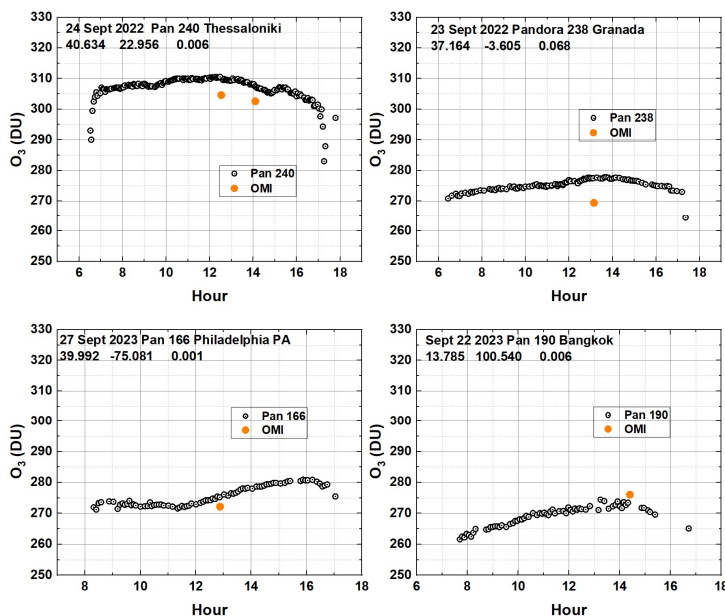


Fig. 13a A comparison of Pandora and OMI retrievals of total column O<sub>3</sub> at the time of the OMI satellite overpass. Local Principal Investigators: Pan 240 Alexander Cede, Pan 238 Inmaculada Foyo Moreno, Pan 166 Lukas Valin, and Pan 190 Surassawadee Phoompan.

The diurnal variation of TCO seen by Pandora can be compared (Fig. 13b) with that observed by the Earth Polychromatic Imaging Camera (EPIC) on the DSCOVR (Deep Space Climate Observatory) satellite orbiting about the Earth-Sun gravitational balance Lagrange-1 point (Herman et al., 2018). EPIC obtains simultaneous data from sunrise to sunset once per hour (once per 90 minutes during Northern



Hemisphere winter) as the Earth rotates in EPIC's FOV (field of view). Examples of EPIC's view of the whole illuminated Earth are available from <https://epic.gsfc.nasa.gov/>. The spatial resolution for TCO is 18 x 18 km<sup>2</sup> at the center of the image (the color images have 10 x 10 km<sup>2</sup> resolution).

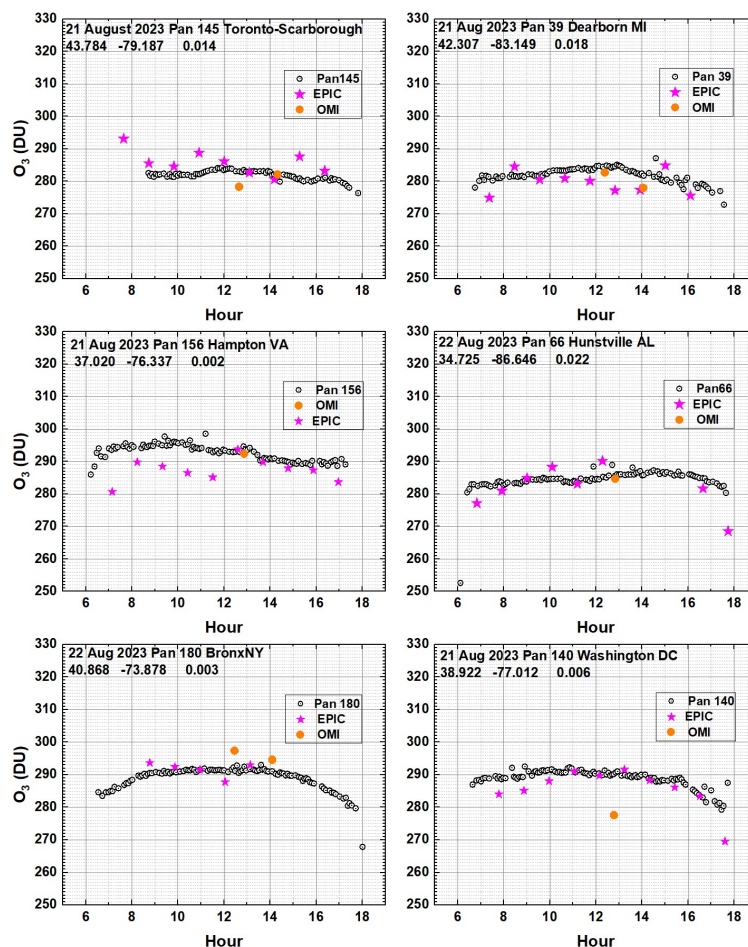


Fig. 13b A comparison of Pandora (Open Circles), EPIC (magenta stars), and OMI (orange circles) retrievals of total column O<sub>3</sub> at the times of the satellite overpasses. Local Principal Investigators: Pan 145 Vitali Fioletov, Pan 66 Lukas Valin, Pan 39 Lukas Valin, Pan 156 Alexander Cede, Pan 66 Nader Abuhassan, Pan180 Lukas Valin, and Pan 140 Jim Szykman

255

256 The TCO values in the early morning and late afternoon are not correctly retrieved for both Pandora and  
 257 EPIC because of the high solar zenith angle exceeding 75°. For the cases shown, the TCO data are  
 258 properly retrieved between 07:00 and 17:00 local solar time. The 10:20 and 11:30 EPIC value for  
 259 Hampton, VA of 286.5 and 285DU differs from Pandora by -3 %. Other differences are smaller.  
 260 Occasionally, OMI differs from Pandora values as is the case, -4.6 %, for 21 August 2023 over  
 261 Washington, DC.



262 **3.0 Summary**

263 Typical examples of the seasonal variability of HCHO, NO<sub>2</sub>, and O<sub>3</sub> in terms of their measured total  
264 column TCHCHO, TCNO<sub>2</sub>, and TCO have been presented from both Pandora Spectrometer instruments  
265 and the OMI spectrometer instrument overpass retrievals of selected Pandora sites. For TCO, an  
266 additional hourly comparison is made with the EPIC instrument located in an orbit about the Earth-Sun  
267 Lagrange-1 point. For most sites, OMI does not observe the strong seasonal variation of TCHCHO that is  
268 clearly seen in the Pandora data. The lack of OMI seasonal variation in TCHCHO at most sites suggests  
269 that OMI is not seeing the lowest layers of the HCHO variation.

270 OMI TCNO<sub>2</sub> at one shown site, Toronto-Scarborough, appears to show seasonal variability that the  
271 Pandora 145 does not see. This could be because OMI is detecting the NO<sub>2</sub> source from winter heating in  
272 the city, while the Pandora site (University of Toronto campus) is fairly remote from Toronto city  
273 buildings and is mostly affected road traffic as the source of NO<sub>2</sub>.

274 A comparison between the multi-year time series of Pandora and OMI TCNO<sub>2</sub> in urban areas shows that  
275 OMI is underestimating the degree of atmospheric pollution. The results for TCNO<sub>2</sub> and TCO agree with  
276 data, 2012 – 2017, from a previous study before the Pandora upgrade (Herman et al., 2019). When  
277 Pandora is limited to an average of data obtained between 13:00 and 14:00 hours, the agreement  
278 between Pandora and OMI TCNO<sub>2</sub> is much better. Comparisons of daily time series TCHCHO and TCNO<sub>2</sub>  
279 with OMI overpass values show agreement about 50 % of the time.

280 Total column ozone agrees well in both seasonal variation and in the comparison with Pandora at the  
281 OMI overpass time. Given the nature of the ozone retrieval algorithm, the good agreement with TCO  
282 suggests that the UV calibrations for both Pandora and OMI are correct. There is good agreement  
283 between Pandora TCO with the hourly TCO obtained from the DSCOVR-EPIC instrument observing the  
284 Earth from an orbit about the Earth-Sun gravitational balance Lagrange-1 point.

285

286



287 **4.0 References**

- 288 Boeke NL, Marshall JD, Alvarez S, Chance KV, Fried A, Kurosu TP, Rappenglück B, Richter D, Walega J,  
289 Weibring P, Millet DB. Formaldehyde columns from the Ozone Monitoring Instrument: Urban versus  
290 background levels and evaluation using aircraft data and a global model, *J. Geophys. Res.* 2011 Mar  
291 16;116(D5):10.1029/2010jd014870, doi: 10.1029/2010jd014870, 2011.
- 292
- 293 Boersma, Klaas & Jacob, D. & Trainic, Miri & Rudich, Yinon & De Smedt, Isabelle & R, Dirksen & Eskes,  
294 Henk, Validation of urban NO<sub>2</sub> concentrations and their diurnal and seasonal variations observed from  
295 space (SCIAMACHY and OMI sensors) using in situ measurements in Israeli cities. *Atmos Chem Phys*, 9.  
296 10.5194/acp-9-3867-2009, 2009.
- 297
- 298 Gratien, A., B. Picquet-Varrault, J. Orphal, E. Perraudin, J.-F. Doussin and J.-M. Flaud, Laboratory  
299 intercomparison of the formaldehyde absorption cross sections in the infrared (1660–1820 cm<sup>-1</sup> and  
300 ultraviolet (300–360 nm) spectral regions, *J. Geophys. Res.*, **112**, <https://doi.org/10.1029/2006JD007201>,  
301 D05305 1-10, 2007.
- 302
- 303 Herman, J., A. Cede, E. Spinei, G. Mount, M. Tzortziou, and N. Abuhassan, NO<sub>2</sub> column amounts from  
304 ground-based Pandora and MFDOAS spectrometers using the direct-sun DOAS technique:  
305 Intercomparisons and application to OMI validation, *J. Geophys. Res.*, 114, D13307,  
306 doi:[10.1029/2009JD011848](https://doi.org/10.1029/2009JD011848), 2009.
- 307
- 308 Herman, J., Huang, L., McPeters, R., Ziemke, J., Cede, A., and Blank, K.: Synoptic ozone, cloud reflectivity,  
309 and erythemal irradiance from sunrise to sunset for the whole earth as viewed by the DSCOVR  
310 spacecraft from the earth sun Lagrange 1 orbit, *Atmos. Meas. Tech.*, 11, 177-194,  
311 <https://doi.org/10.5194/amt-11-177-2018>, 2018.
- 312
- 313 Herman, J., Abuhassan, N., Kim, J., Kim, J., Dubey, M., Raponi, M., and Tzortziou, M.: Underestimation of  
314 column NO<sub>2</sub> amounts from the OMI satellite compared to diurnally varying ground-based retrievals from  
315 multiple PANDORA spectrometer instruments, *Atmos. Meas. Tech.*, 12, 5593–5612,  
316 <https://doi.org/10.5194/amt-12-5593-2019>, 2019.
- 317
- 318 Judd LM, Al-Saadi JA, Valin LC, Pierce RB, Yang K, Janz SJ, Kowalewski MG, Szykman JJ, Tiefengraber M  
319 and Mueller M (2018) The Dawn of Geostationary Air Quality Monitoring: Case Studies From Seoul and  
320 Los Angeles. *Front. Environ. Sci.* 6:85. doi: 10.3389/fenvs.2018.00085, 2018.
- 321
- 322 Morfopoulos C, Müller J-F, Stavrakou T, et al. Vegetation responses to climate extremes recorded by  
323 remotely sensed atmospheric formaldehyde. *Glob Change Biol.*, 28, 1809–1822.  
324 <https://doi.org/10.1111/gcb.15880>, 2021.
- 325
- 326 Newmark, G. (2001). Emissions Inventory Analysis of Mobile Source Air Pollution In Tel Aviv, Israel,  
327 Transportation Research Record, Vol. 1750, p. 40-48, <https://doi.org/10.3141/1750-0>, 2001.
- 328
- 329 Peng, W.-X., X.-C. Yue, H.-L. Chen, N.L. Ma, Z. Quan, Q. Yu, C. Sonne, A review of plants formaldehyde  
330 metabolism: Implications for hazardous emissions and phytoremediation, *J. Hazard. Mater.* 436 Article  
331 129304, <https://doi.org/10.1016/j.jhazmat.2022.129304>, 2022.



- 332 Spinei, E., Whitehill, A., Fried, A., Tiefengraber, M., Knepp, T. N., Herndon, S., Herman, J. R., Müller, M.,  
333 Abuhassan, N., Cede, A., Richter, D., Walega, J., Crawford, J., Szykman, J., Valin, L., Williams, D. J., Long,  
334 R., Swap, R. J., Lee, Y., Nowak, N., and Poche, B.: The first evaluation of formaldehyde column  
335 observations by improved Pandora spectrometers during the KORUS-AQ field study, *Atmos. Meas. Tech.*,  
336 11, 4943–4961, <https://doi.org/10.5194/amt-11-4943-2018>, 2018.
- 337 Spinei, E., Tiefengraber, M., Müller, M., Gebetsberger, M., Cede, A., Valin, L., Szykman, J., Whitehill, A.,  
338 Kotsakis, A., Santos, F., Abuhassan, N., Zhao, X., Fioletov, V., Lee, S. C., and Swap, R.: Effect of  
339 polyoxymethylene (POM-H Delrin) off-gassing within the Pandora head sensor on direct-sun and multi-  
340 axis formaldehyde column measurements in 2016–2019, *Atmos. Meas. Tech.*, 14, 647–663,  
341 <https://doi.org/10.5194/amt-14-647-2021>, 2021.
- 342 Stavrakou, T., Müller, J.-F., Bauwens, M., Boersma, K. F. & van Geffen, J. Satellite evidence for changes in  
343 the NO<sub>2</sub> weekly cycle over large cities. *Sci. Rep.* <https://doi.org/10.1038/s41598-020-66891-0> (2020).
- 344 Tzortziou, M., Herman, J.R., Cede, A. *et al.* Spatial and temporal variability of ozone and nitrogen dioxide  
345 over a major urban estuarine ecosystem. *J Atmos Chem* **72**, 287–309, [https://doi.org/10.1007/s10874-](https://doi.org/10.1007/s10874-013-9255-8)  
346 [013-9255-8](https://doi.org/10.1007/s10874-013-9255-8), 2015.
- 347 Van der A, R. J., H. J. Eskes, K. F. Boersma, T. P. C. van Noije, M. Van Roozendaal, I. De Smedt, D. H. M. U.  
348 Peters, and E. W. Meijer, Trends, seasonal variability and dominant NO<sub>x</sub> source derived from a ten year  
349 record of NO<sub>2</sub> measured from space, *J. Geophys. Res.*, 113, D04302, doi:10.1029/2007JD009021, 2008.
- 350 Wang, P.; Holloway, T.; Bindl, M.; Harkey, M.; De Smedt, I. Ambient Formaldehyde over the United  
351 States from Ground-Based (AQS) and Satellite (OMI) Observations. *Remote Sens.* 14, 2191,  
352 <https://doi.org/10.3390/rs14092191>, 2022.
- 353 Wittrock, F., Richter, A., Oetjen, H., Burrows, Wittrock, F., Richter, A., Oetjen, H., Burrows, J. P., Kanakidou,  
354 Myriokefalitakis, S., Volkamer, R., Beirle, S., Platt, U., and Wagner, T.: Simultaneous global observations of  
355 glyoxal and formaldehyde from space, *Geophys. Res. Lett.*, 33, L16804,  
356 <https://doi.org/10.1029/2006GL026310>, 2006.
- 357 Zhang, Y., Li, R., Min, Q., Bo, H., Fu, Y., Wang, Y., & Gao, Z. (2019). The controlling factors of atmospheric  
358 formaldehyde (HCHO) in Amazon as seen from satellite. *Earth and Space Science*, 6, 959–971.  
359 <https://doi.org/10.1029/2019EA000627>, 2019.





361 **Author contribution:**

362 Jay Herman is responsible for writing the paper and creating the figures. Jianping Mao obtained the  
363 EPIC overpass data for the Pandora sites and discussed aspects of the paper.

364 **Data Availability**

365 Worldwide Pandora data for 63 sites can be freely downloaded from the Austrian Pandonia website  
366 <https://data.pandonia-global-network.org/> or from a NASA backup site updated every week.

367 [https://avdc.gsfc.nasa.gov/pub/DSCOVER/Pandora/DATA\\_02/](https://avdc.gsfc.nasa.gov/pub/DSCOVER/Pandora/DATA_02/)

368 The OMI overpass TCHCHO and TCNO2 data are found at

369 <https://avdc.gsfc.nasa.gov/pub/data/satellite/Aura/OMI/V03/L2OVP/OMHCHO/>.

370 <https://avdc.gsfc.nasa.gov/pub/data/satellite/Aura/OMI/V03/L2OVP/OMNO2/>

371 OMI TCO overpass data are available from

372 <https://avdc.gsfc.nasa.gov/pub/data/satellite/Aura/OMI/V03/L2OVP/OMTO3/>

373

374 **Competing interests:**

375 The authors declares that they have no conflicts of interest.

376

377 Funding: This study is funded by the DSCOVER-EPIC project through the University Of Maryland  
378 Baltimore County

379

380 **Acknowledgements:**

381 The authors want to acknowledge the contribution of each of the Pandora Principal Investigators  
382 included in the figure captions and for the OMI team and Dr. Lok Lamsal for making OMI overpass  
383 data available. Acknowledgement is also due to the Pandonia team lead by Dr. Alexander Cede for  
384 processing all of the Pandora data and devising the retrieval algorithms and to Dr. Nader Abuhassan  
385 for building and calibrating all of the Pandora spectrometer systems.

386





387 **Figure Captions**

388 Fig. 1 Seasonal and daily behavior of HCHO and NO<sub>2</sub> from Pan 180 located in the Bronx, NYC at 40.868°N,  
389 -73.878°W. The red line is a Lowess(0.03) fit to the data, which is approximately a 1-month local least-  
390 squares average. The Local principal investigator for Pan 180 is Dr. Luke Valin.

391 Fig. 2 The daily average seasonal variation of HCHO and NO<sub>2</sub> over Fordham University in Bronx, New  
392 York City from Pandora 180 at 40.868° latitude and -73.878° longitude. Each point is a daily average of  
393 the data in Fig.1. Local principal investigator: Dr. Luke Valin

394 Fig. 3 The seasonal variation of TCHCHO and TCNO<sub>2</sub> over New Haven Connecticut from Pandora 64 at  
395 41.301°N latitude and -72.903°W longitude. Each point is a daily average. Local principal investigator:  
396 Dr. Nader Abuhassan.

397 Fig. 4 The seasonal variation of TCHCHO and TCNO<sub>2</sub> over equatorial Bangkok Indonesia at 13.785°N and  
398 100.540°E. The local principal investigator is Surassawadee Phoompanit.

399 Fig. 5 Seasonal variation in daily average TCHCHO and TCNO<sub>2</sub> in Tel Aviv Israel from Pandora 182 located  
400 at 32.113°N 34.085°E at a height of 8 meters. The local principal investigator for Pan 182 is Dr. Michal  
401 Rozenhaimer.

402 Fig. 6 Seasonal variation in daily average HCHO and NO<sub>2</sub> in Wakkerstroom South Africa from Pandora  
403 159 located at -27.359°S and 30.144°E. Local principal investigator: B. Scholes

404 Fig. 7 Comparison of OMI (approximately 13:30) and Pandora (09:00 – 16:00) total column NO<sub>2</sub> time  
405 series in Bronx NY (40.868°N, -73.878°W) and Busan Korea (35.235°N, 129.083°E). Local principal  
406 investigator for Pan20 is Jae Hwan Kim and for Pan 180 is Dr. Luke Valin

407 Fig. 8 A comparison between Pandora and OMI (purple circle) total column NO<sub>2</sub>. The Local principal  
408 investigator for Pan 180 is Dr. Luke Valin and for Pan 20 is Dr. Jae Hwan Kim.

409 Fig. 9 A comparison between Pandora and OMI (purple circle) total column HCHO. The Local principal  
410 investigator for Pan 180 is Dr. Luke Valin and for Pan 20 is Dr. Jae Hwan Kim.

411 Fig. 10a A comparison of Pandora TCHCHO and TCNO<sub>2</sub> daily average total column amounts for Toronto-  
412 Scarborough University of Toronto and OMI data for Toronto East (43.740°N, -79.270°W at  
413 approximately 14:20 Local Standard Time). The local principal investigator for Pan 145 is Dr. Vitali  
414 Fioletov.

415 Fig. 10b The same as Fig. 10a but for all the Pandora data.

416 Fig. 11 A comparison of OMI Total Column Ozone values with those obtained from Pandora 140 over the  
417 Washington DC site at 38.922°N and -77.012°W. The local principal investigator for Pan 140 is Dr. Jim  
418 Szykman.

419 Fig. 12 A comparison of OMI Total Column Ozone values with those obtained from Pandora 20 over the  
420 Busan, Korea site at 32.325°N and 129.083°E. The local principal investigator for Pan20 is Jae Hwan Kim.



421 Fig. 13a A comparison of Pandora and OMI retrievals of total column O<sub>3</sub> at the time of the OMI satellite  
422 overpass. Local Principal Investigators: Pan 240 Alexander Cede, Pan 238 Inmaculada Foyo Moreno, Pan  
423 166 Lukas Valin, and Pan 190 Surassawadee Phoompan.

424 Fig. 13b A comparison of Pandora (Open Circles), EPIC (magenta stars), and OMI (orange circles)  
425 retrievals of total column O<sub>3</sub> at the times of the satellite overpasses. Local Principal Investigators: Pan  
426 145 Vitali Fioletov, Pan 66 Lukas Valin, Pan 39 Lukas Valin, Pan 156 Alexander Cede, Pan 66 Nader  
427 Abuhassan, Pan180 Lukas Valin, and Pan 140 Jim Szykman.

428

429